Supplementary data

BMI-1 targeting interferes with patient-derived tumor-initiating cell survival and tumor growth in prostate cancer. Nitu Bansal, Monica Bartucci, Shamila Yusuff, Stephani Davis, Kathleen Flaherty, Eric Huselid, Michele Patrizii, Daniel Jones, Liangxian Cao, Nadiya Sydorenko, Young-Choon Moon, Hua Zhong, Daniel J. Medina, John Kerrigan, Mark N. Stein, Isaac Y. Kim, Thomas W. Davis, Robert S. DiPaola, Joseph R. Bertino, Hatem E. Sabaawy

Supplementary Figures

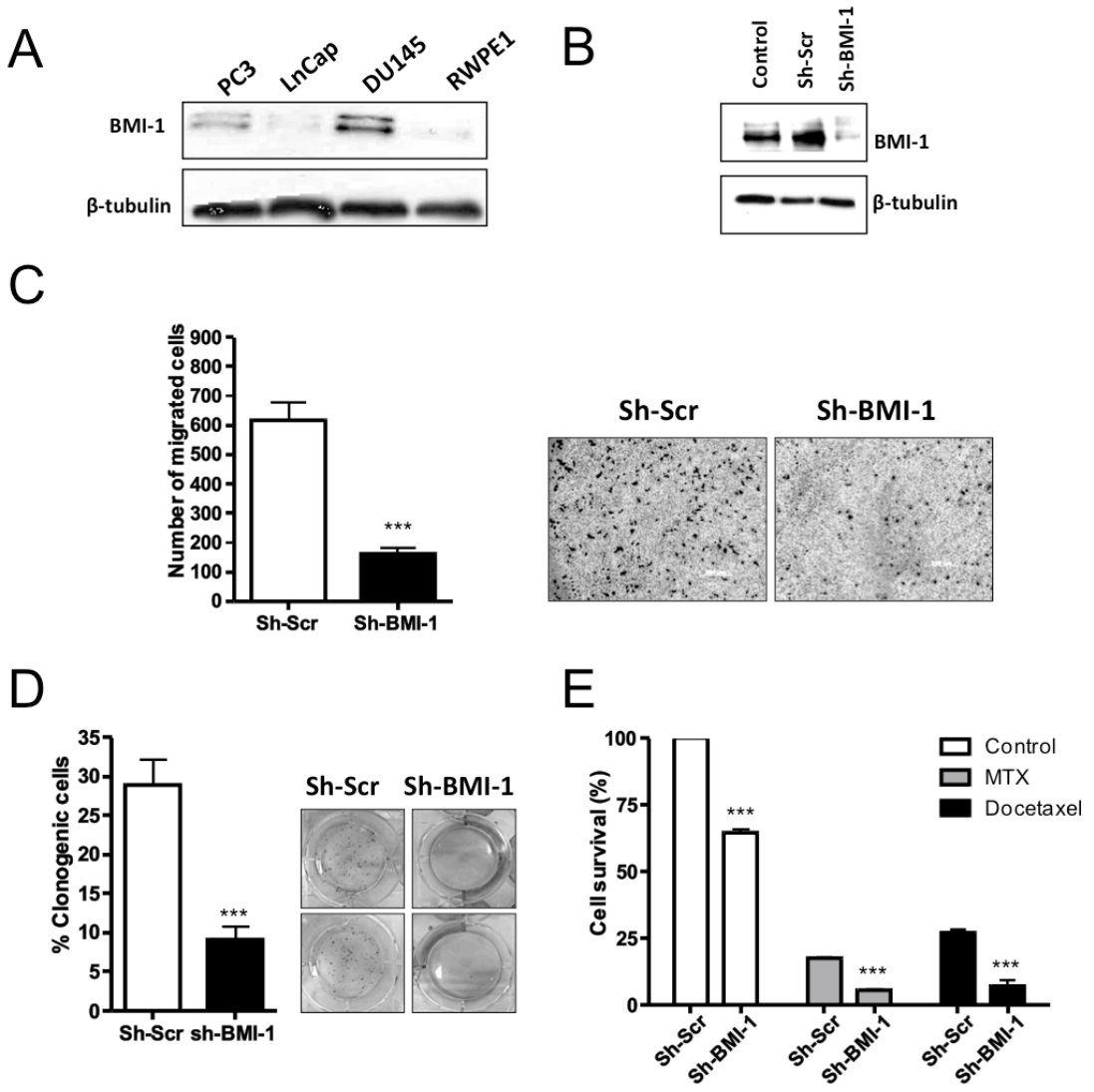

Figure S1. Functional role(s) of BMI-1 in PCa. *A*, Western Blot analysis for BMI-1 expression in prostate cancer cell lines (PC3, LNCap, and DU145), and in immortalized normal prostate epithelial cells (RWPE-1). *B*, Western blot analysis for BMI-1 expression in cell lysates from untransduced DU145, control vector-transduced (Sh-Scr) and BMI-1-depleted (shBMI-1) cells. β-tubulin was used to assess equal loading. *C*, Left: Graph showing the number of migrated cells in standard growth conditions. For the migration assay, 20.000 DU145 Sh-Scr and sh-BMI-1 cells were plated in modified Boyden chambers. Migrated cells were stained with Comassie Blue and counted under the microscope after 96h (Scale bars 200μm). A representative image is shown (right panel). Graph is showing the outcome of three independent experiments. *D*, Percentage of clonogenic cells upon BMI-1 knockdown compared to sh-Scr control. Images on the right demonstrate colonies stained with crystal violet. *E*, Percentage of cell survival upon combined knockdown of BMI-1 and treatment with chemotherapeutic agent methotrexate (MTX, 10nM) or docetaxel (2.5 nM) compared to DMSO controls. Results are shown as mean ± S.D. of three independent experiments. ***P*-value <0.01, ****P*-value <0.001.

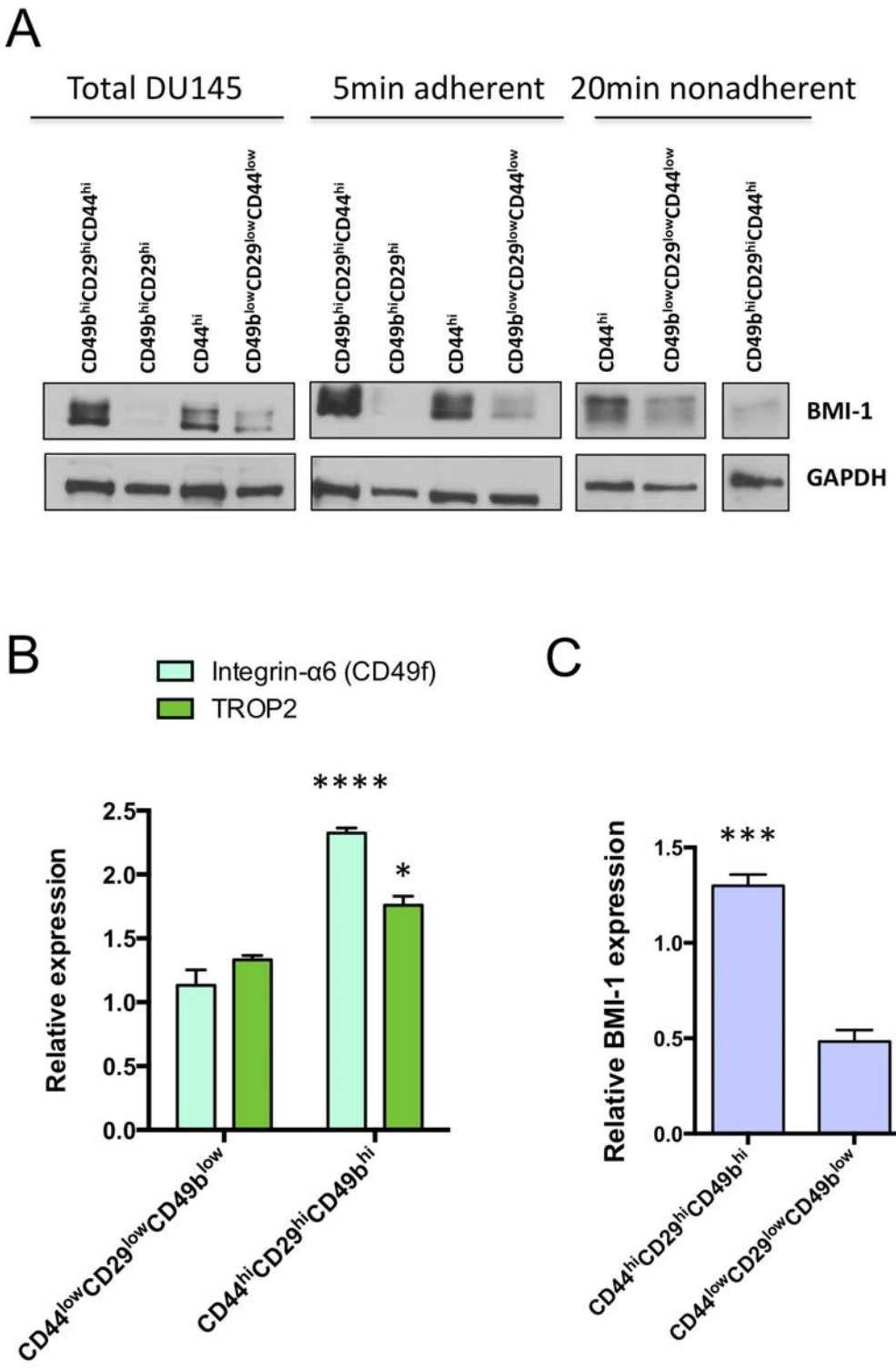

Figure S2. BMI-1 expression in subpopulations of DU145 cells. *A*, Western blot analysis for BMI-1 expression in subpopulations of adherent, nonadherent and/or sorted DU145 cells. GAPDH was used for equal loading. *B*, Q-PCR analyses of CD49f (integrin-α6) and TROP2 in subpopulations of DU145 cells. *C*, Q-PCR analyses of BMI-1 in subpopulations of DU145 cells. Comparison of the differences in relative expression between each subpopulation and total $CD49b^{low}CD29^{low}CD44^{low}$ DU145 cells was determined using Mann-Whitney U test. Graph indicates significant enrichment of CD49f (****$p<0.0001$) TROP2 (*$p<0.05$) in *B* and BMI-1 (***$p<0.001$) in *C*, in the 5min adherent $CD49b^{hi}CD29^{hi}CD44^{hi}$ cells *vs.* $CD49b^{low}CD29^{low}CD44^{low}$ DU145 cells. Results are shown as mean ± S.D. of 3 independent experiments.

A

Drugs	IC_{50}
Doxorubicin	50 nM
Docetaxel	2.5 nM
Methotrexate	10 nM
C-206	1.5 μM
C-207	1 μM
C-208	1 μM
C-209	2 μM
C-210	10 nM
C-211	1 μM
C-212	10 nM

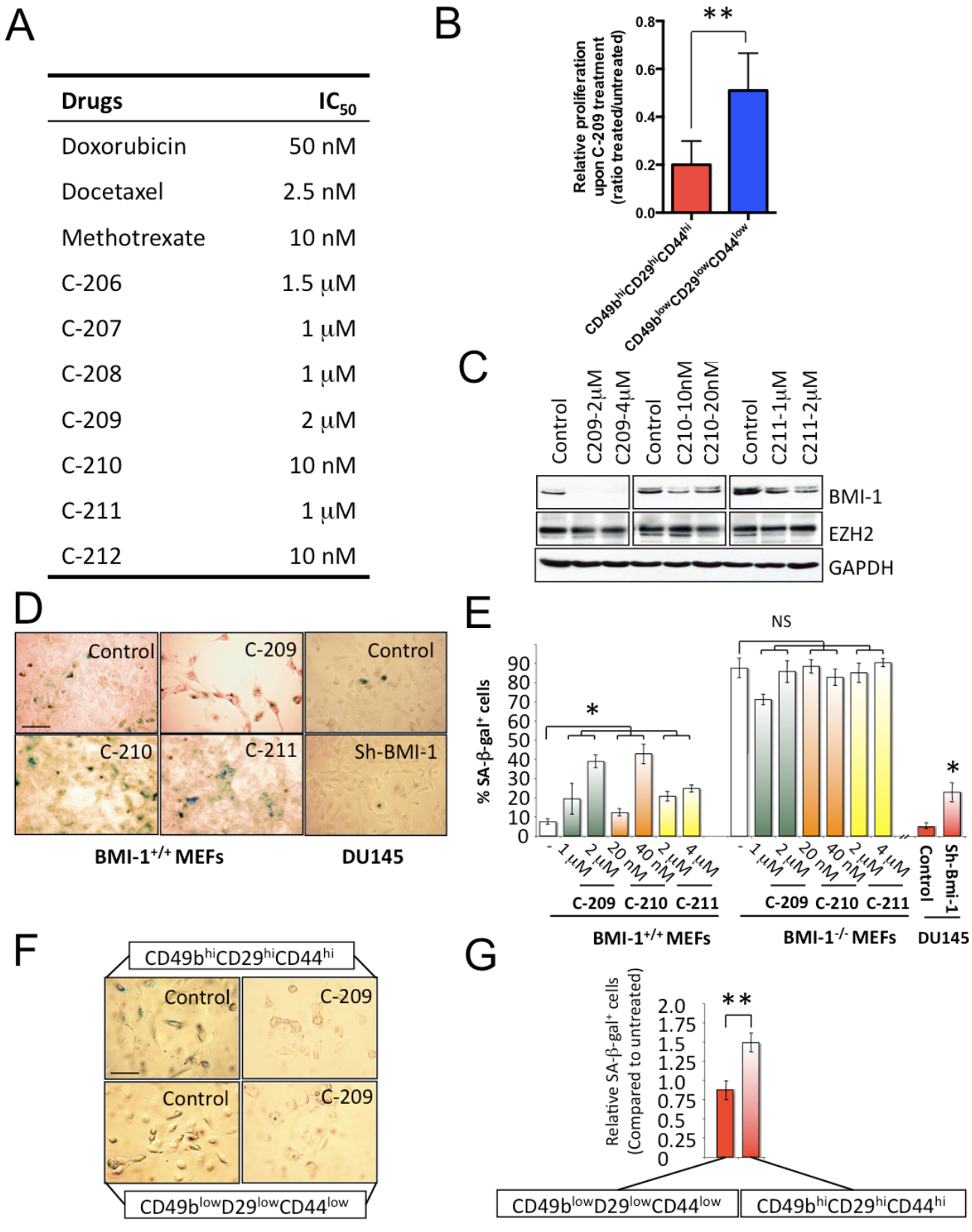

Figure S3. Pharmacological inhibition of BMI-1. *A*, IC_{50} concentrations of doxorubicine, methotrexate, docetaxel and Bmi-1 inhibitors C-206 to C-212. IC_{50}s were determined using MTS assays on DU145 cells. *B*, Cell viability of CD49bCD29CD44^{hi} (TIC) vs. CD49bCD29CD44^{low} cells upon C-209 treatment. *C*, Western blot analysis showing BMI-1

and EZH2 expression levels in DU145 cells treated for 72 hours with C-209, C-210 and C-211 at 1x and 2x of the IC_{50} concentrations. GAPDH levels were used as controls. *D*, SA-β-gal staining of mouse embryonic fibroblasts (MEFs) and DU145 cells treated for 72h with C-209, C-210, or C-211 IC_{50}s. The reduced cell density in the image after treatment with C-209 is due to significant killing of PCa cells. *E*, Quantitation of SA-β-gal staining in control and C-209-, C-210-, or C-211-treated MEFS with (Bmi-$1^{+/+}$) or without Bmi-1 expression (Bmi-$1^{-/-}$), and in sh-Bmi-1 targeted DU145 cells. Note that Bmi-1-null MEFs have high levels of senescence. (*p<0.01 compared to untreated cells, NS, not significant). *F*, SA-β-gal staining of sorted DU145 CD49bCD29CD44 ^{hi} *vs* ^{low} cells treated for 72h with C-209 at IC_{50}. *G*, Quantitation of SA-β-gal staining in control and C-209-treated sorted DU145 cells displayed as a normalized ratio to the number of SA-β-gal positive cells in untreated cells. Scale bar is 50 μm.

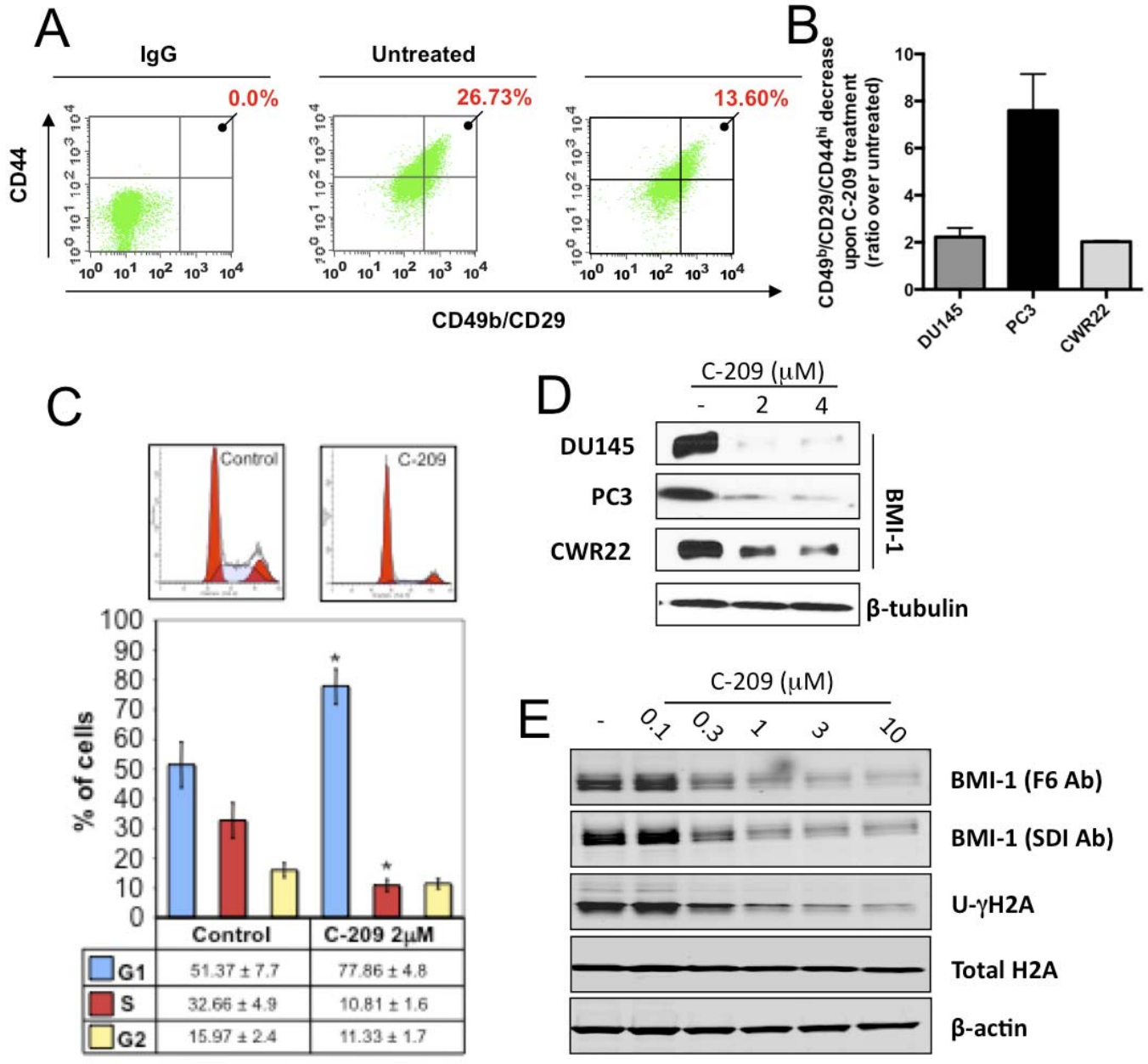

Figure S4. Molecular and cellular effects of pharmacological targeting of BMI-1. *A*, Representative cytofluorimetric analysis showing reduction of $CD49b^{hi}CD29^{hi}CD44^{hi}$ prostate TICs upon C-209 treatment. DU145 cells were treated with C-209 (2μM) for 72 hours. These cells were then stained, and examined using flow cytometry and Cell Quest software.

The mean percentages of TICs population in untreated DU145 are 24.25%, 10.85% in PC3 and 0.02% in CWR22. *B*, Graphical representation showing impaired percentage of $CD49b^{hi}CD29^{hi}CD44^{hi}$ TIC phenotype in DU145, PC3 and CWR22 cells following C-209 treatment. Data are displayed as mean ± S.D. of three independent experiments. *C*, Cell cycle analyses assessed on DU145 cells treated with C-209 (2μM) for 72hrs. In bottom panel, results are shown as mean ± S.D. of three independent experiments. *D*, BMI-1 expression levels in DU145, PC3 and CWR22 PCa cells treated with increasing concentrations of C-209 (indicated). β-tubulin (shown only from DU145 cells) was used as loading control. *E*, The expression of BMI-1 using two different antibodies (Targeting the full-length of the protein (F6 Ab) or the carboxyl terminal (SDI Ab)) in response to C-209. Notice the dose-dependent reduction of the C-terminal lysine-119 mono-ubiquitinated form of γ-H2A (U), a specific product of the BMI-1/PRC1 complex, compared to total H2A and β-actin.

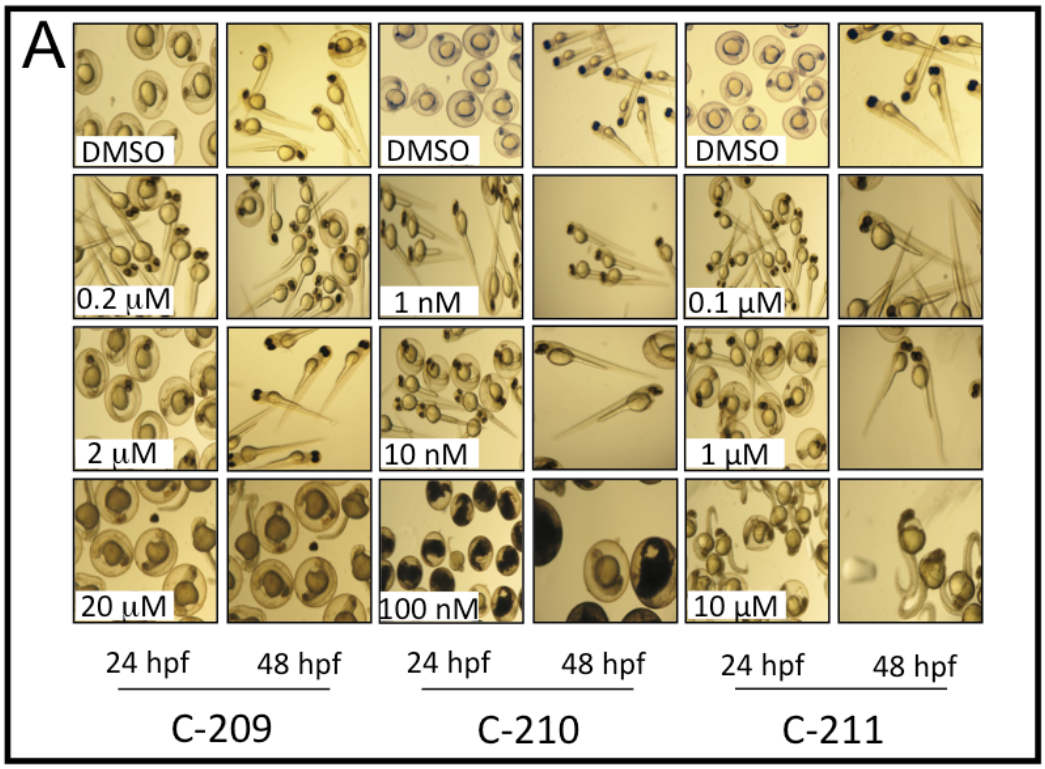

B **Survival of zebrafish embryos after treatment with BMI-1 inhibitors (%)**

	DMSO	C-209 (μM)			C-210 (nM)			C-211 (μM)		
		0.2	2	20	1	10	100	0.1	1	10
24 hpf	98 ± 1	97 ± 1	98 ± 1	90 ± 3	98 ± 1	96 ± 4	0	99 ± 1	98 ± 1	0
48 hpf	98 ± 1	98 ± 1	97 ± 2	65 ± 4	97 ± 1	90 ± 4	0	98 ± 1	98 ± 1	0

Figure S5. Examining BMI-1 inhibitors in toxicological assays and effects on normal cells. *A*, Bright field images of zebrafish embryos treated with BMI-1 inhibitors at the indicated concentrations, and compared to vehicle treatment with DMSO. Progress in normal embryonic development is indicated by hatching of the embryos outside of the surrounding chorionic shell, typically occurring at 48-72 hour post-fertilization (hpf). The dark areas indicate necrotic tissues due to toxic effects. *B*, Survival of zebrafish embryos after 24 and 48 hpf. In each treatment, at least 50 embryos were employed. Survivals are presented as mean percentage ± S.D. from three independent experiments. Compounds were dissolved in DMSO and added to embryo water starting at 12 hpf.

A

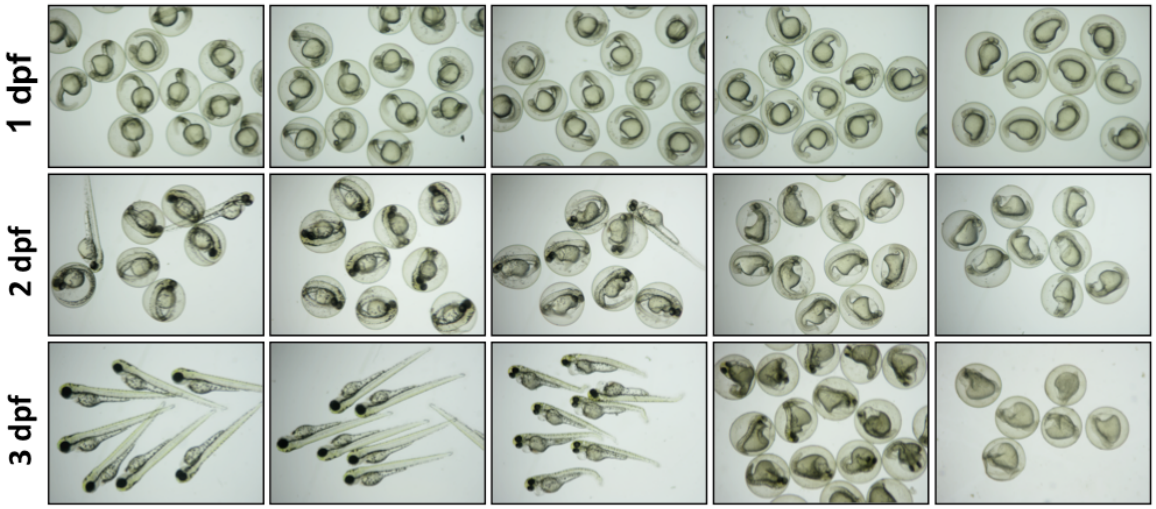

Survival of zebrafish embryos after treatments (%)

	DMSO	C-209 3μM	CHX 1μg/ml	CHX 5μg/ml	CHX 10μg/ml
24 hpf	98± 0.6	98± 0.6	98± 0.6	98± 0.6	98± 1
48 hpf	98± 0.6	98± 0.0	98± 0.6	0	0
72 hpf	98± 0.6	98± 0.0	97± 0.6	0	0

B

Survival of adult zebrafish after treatments (%)

	Controls	209 2μM	CHX 1μg/ml	CHX 5μg/ml	CHX 10μg/ml
24 hpt	100	100	100	0	0
48 hpt	100	100	100	0	0
72 hpt	93	100	90	0	0

Figure S6. Toxicity effects of C-209 and CHX on adult and embryo zebrafish. *A*, Upper panel: Bright field images of zebrafish embryos treated with Cycloheximide (CHX), C-209, or DMSO at the indicated concentrations. Compounds were added to embryo water at 12 hours post-fertilization (hpf) to examine the effects on embryo development and survival for 3 days. CHX treated embryos displayed toxic effects such as cardiac edema and curling of tails by 3dpf at the dose of 1 μg/ml. DMSO control and C-209 treated embryos appeared normal at 3dpf (days post-fertilization). At 5 μg /ml CHX, embryos appear mostly normal at 1dpf, but then die by 2dpf as determined by lack of a beating heart. At 10 μg/ml CHX, embryos demonstrate the developmental growth arrest sooner 18hpf to 1dpf, and are dead by 2dpf. At least 20 embryos were used per treatment. Lower panel: Survival table presented as mean percentage ± S.D. from three independent experiments. *B*, Survival table of 6-10 week old zebrafish. A 12-well plate containing 4ml of treatment water and 2 fish per well was incubated at the normal fish maintenance temperature of 28.5 C for three days. Treatment water was changed daily due to accumulation of debris in the wells. The controls include untreated water, 0.5% DMSO, and 0.5% Ethanol. Ten fish per group were used in two independent experiments.

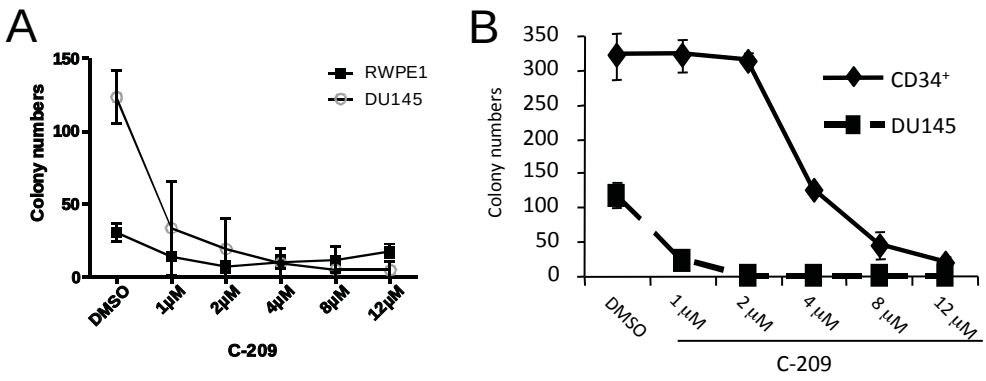

C

Mice peripheral blood hematological profile following C-209 treatment

	CTRL			C-209		
	Mean	**±**	**SD**	**Mean**	**±**	**SD**
WBC (x10^3/μL)	1.22	±	0.92	1.34	±	0.53
Neutrophils	78.40	±	8.26	77.40	±	7.83
Lymphocytes	13.20	±	5.54	13.60	±	5.90
Monocytes	4.20	±	3.35	3.20	±	2.49
Eosinophils	3.60	±	4.34	5.20	±	4.38
Basophils	0.60	±	0.89	0.60	±	0.89
RBC (x10^6/μL)	7.30	±	0.44	6.76	±	0.34
Hemoglobin	11.97	±	0.99	11.06	±	0.88
PLT (x10^3/μL)	883.33	±	472.35	1442.20	±	136.92

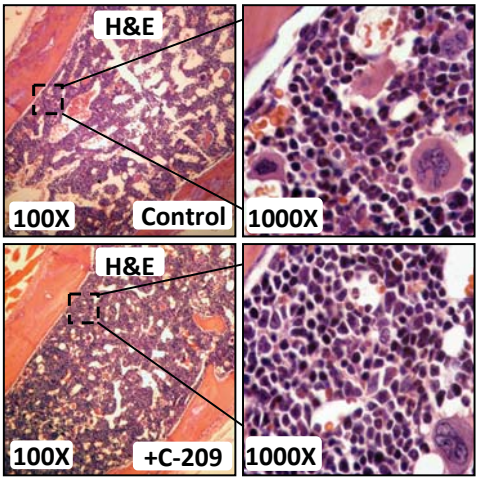

Figure S7. BMI-1 inhibition effect on the normal prostate and hematopoietic system. *A*, Normal epithelial RWPE1 and tumoral DU145 prostate cells were treated with the indicated concentration of C-209 for 72h. Subsequently, cells were collected, counted and 200 cells for each condition were plated to assess colony-forming efficiency. Data plotted represent four independent experiments ($p<0.0001$ between DMSO and 1-12 μM in DU145 cells, NS between DMSO and 1-12 μM in RWPE1 cells). *B*, Human $CD34^+$ cells grown in methocult for hematopoietic colony assays and 200 DU145 cells were plated in 6-well tissue culture dishes and treated in parallel with C-209 at the indicated concentrations. Colony counts represent three independent experiments ($p<0.0001$ at 1-4 μM). *C*, Upper panel: Peripheral blood parameters of C-209-untreated and -treated mice (C-209 60mg/kg/day for ~2 weeks). All mice survived treatments with no apparent phenotypic changes. Peripheral blood was obtained from cardiac puncture bleeding and analyzed within 4hrs from mice sacrifice. N=9 mice/group were analyzed. Student's t-test comparing CRTL and C-209 treated mice indicates no significant differences between the two groups. Lower panel: hematoxylin/eosin staining of bone marrow biopsy sections from the femur derived at day 14 from the treated and untreated (Control) mice. Notice the similar cellularity of the bone marrow of the treated and control mice. The smears demonstrated the presence of heterogeneous cell types including the larger megakaryocytic lineages. Representative images were taken with 10× and 100x objectives.

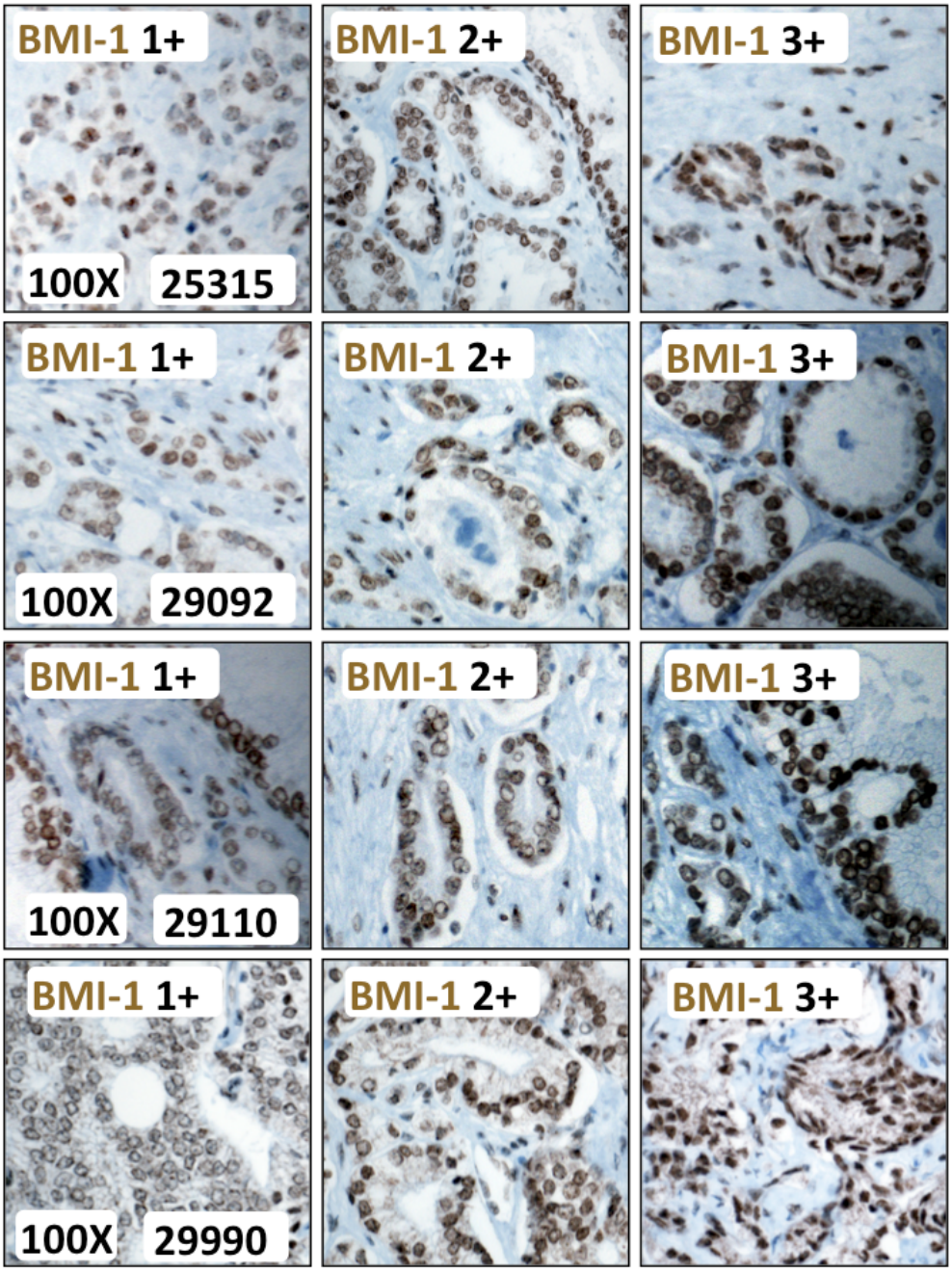

Figure S8. Representative images of BMI-1 expression in primary PCa samples. BMI-1 expression was assessed as the extent of nuclear immunoreactivity by IHC. Score values for BMI-1 levels were: number of BMI-1 strongly staining nuclei (3+), number of BMI-1 moderately staining nuclei (2+), and number of BMI-1 weakly staining nuclei (1+). For each of the 4 representative patient derived tissues, heterogeneity of BMI-1 expression was observed.

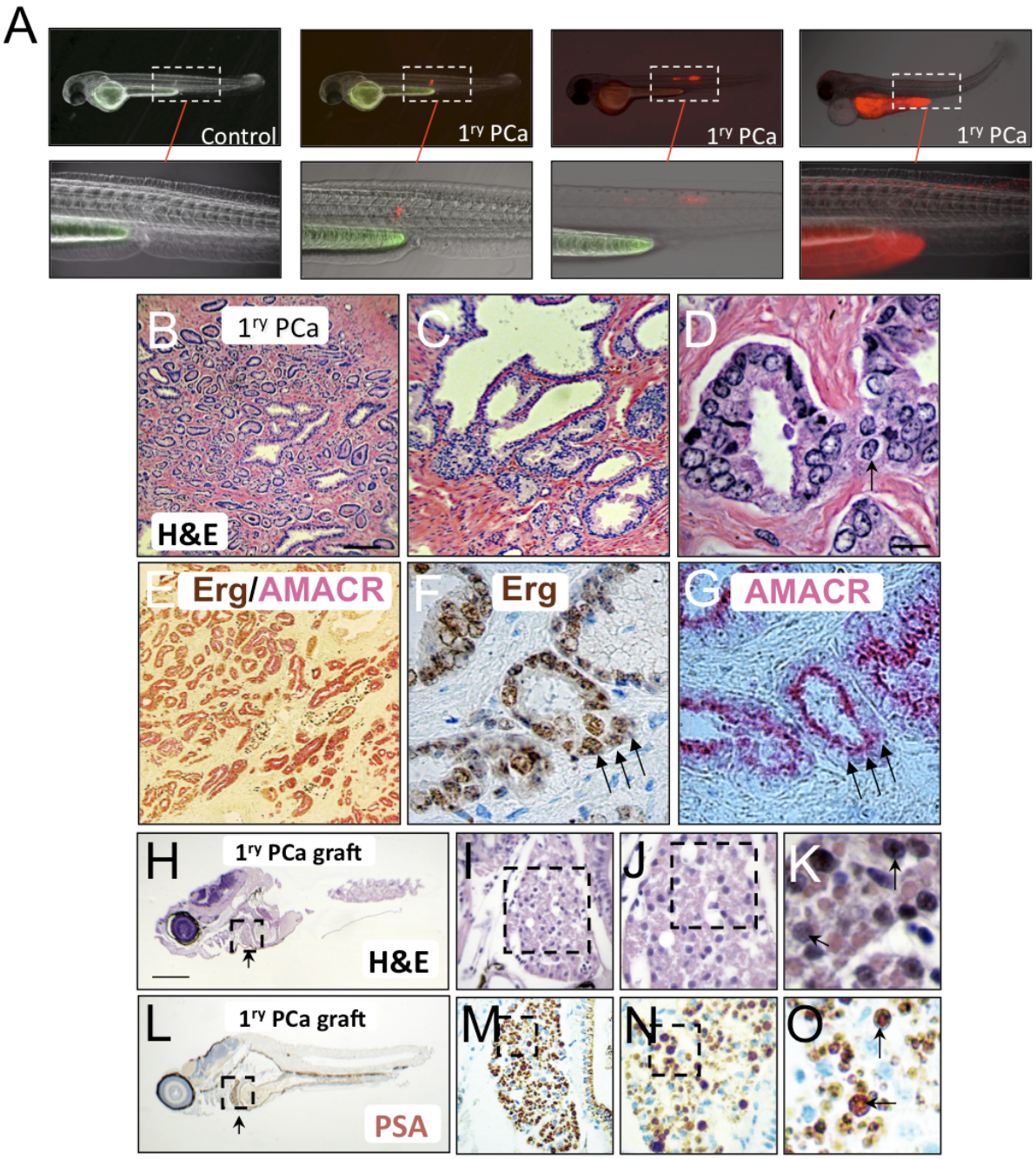

Figure S9. Xenografts of human primary PCa cells in embryonic zebrafish. *A*, Representative images of vehicle-, and QD-labeled primary CD49b^{hi}CD29^{hi}CD44^{hi} engrafted cells. Images are overlays of bright, GFP and red 605 fluorescent images at 4 days post-transplantation (dpt). *B-D*, Histological sections from prostate cancer patient #24126 stained with H&E. Notice the morphology of the cells in *D* (arrow). *E-G*, Formalin fixed paraffin embedded (FFPE) sections from a representative primary PCa tissue used that are stained with dual IHC or single IHC for Erg (in brown) or AMACR (in pink) showing identical expression pattern of both tumor markers (arrows). *H-K*, Histological sections from a representative zebrafish xenograft at 8 dpt demonstrating tumor growth (arrow in *I*). *J-K*, higher magnification of the tumor area in *I*. Notice that the morphology of the cells in *K* (arrows) is identical to the primary tissue sample in *D*. *L-O*, IHC staining of the section in m showing expression of PSA in cells (arrow) of primary PCa fish xenografts. Scale bars are 250 μm in *B*, *E*, *H*, and 10 μm in *D*, *F*, *G*, *K* and *O*.

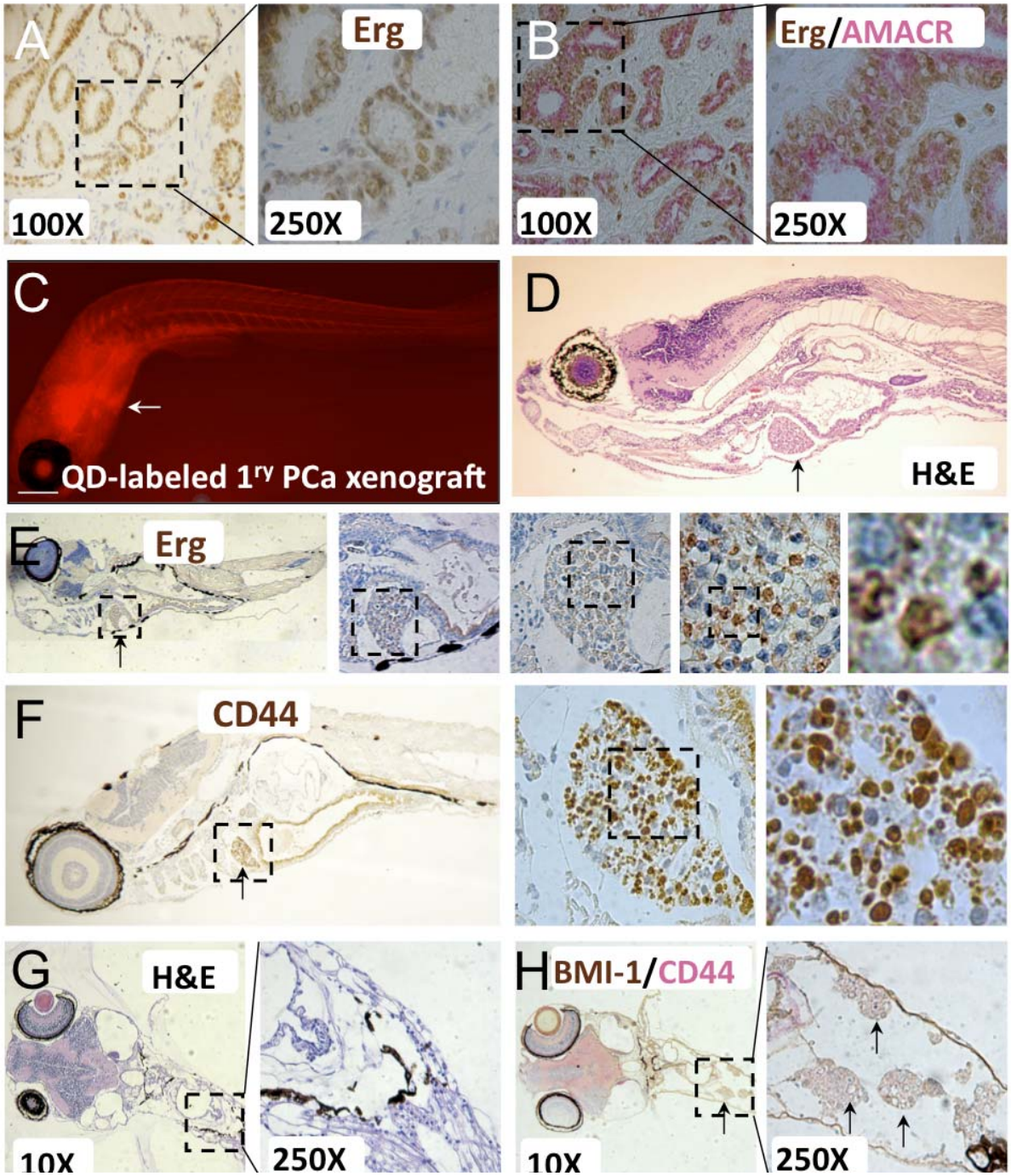

Figure S10. Xenografts of primary PCa tissue in zebrafish embryos. *A*, Section from primary PCa tissue identified to harbor the TEMPRESS-Erg fusion by FISH (not shown) demonstrates overexpression of Erg (brown) by IHC. *B*, Co-localization of Erg (brown) and AMACR (pink) in PCa glands demonstrated by dual IHC staining. *C*, Representative embryos transplanted with quantum-dot (QD) labeled primary PCa cells showing tumor formation as measured by red fluorescence at the 605 QD filter. *D*, Histological sections from a representative zebrafish embryo at 8 days post-transplantation (dpt). *E*, IHC demonstrating expression of Erg in the tumor graft cells (arrow in with higher magnifications in the right panels). *F*, A representative zebrafish embryo at 12 dpt of the mirrorimages of primary cells in a demonstrating expression of CD44 in the tumor graft cells (arrow in with higher magnifications in the right panels). *G-H*, Co-expression of CD44 and BMI-1 in the tumor graft cells (outlined areas in *G* and arrows in *H*). Scale bars are 250 μm in *C*, *D*, *F*, and 100 μm in *E* and *G-H*.

A

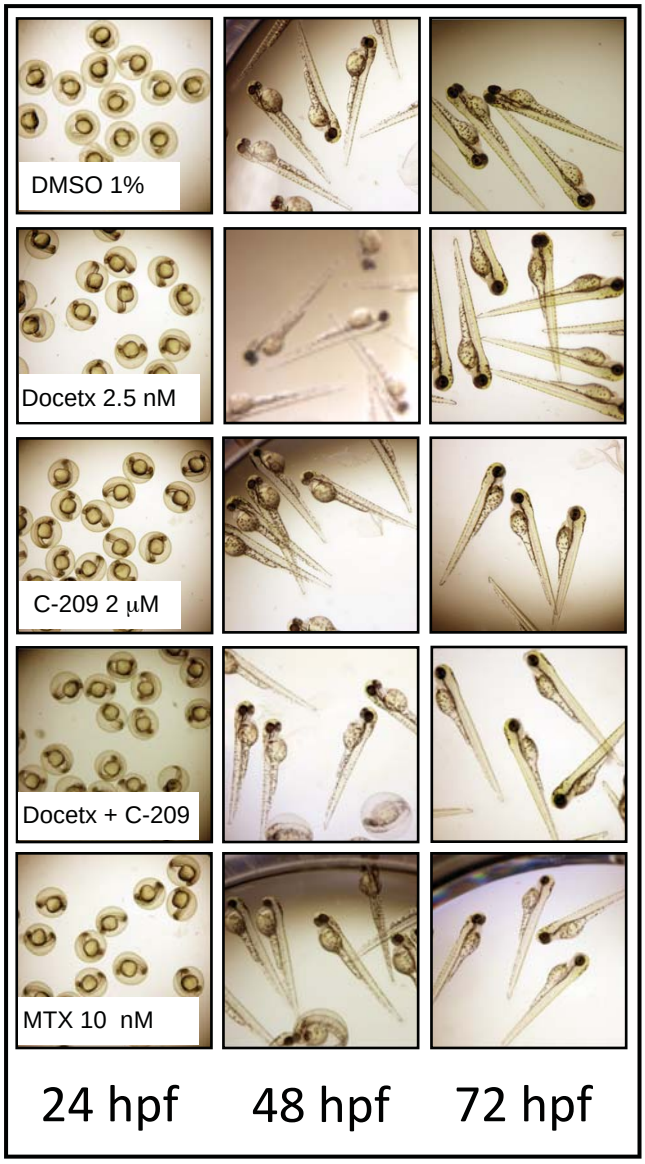

B

Survival of adult zebrafish after treatments (%)

	1% DMSO	MTX	Docetaxel	C-209 2μM	Docetx+ C-209
24 hpf	**100**	**100**	**100**	**100**	**100**
48 hpf	**100**	**100**	**100**	**100**	**100**
72 hpf	**100**	**100**	**100**	**100**	**100**

Figure S11. Toxicology assays of chemotherapy and BMI-1 inhibitors in embryonic zebrafish. *A*, Bright field images of zebrafish embryos treated with chemotherapy and BMI-1 inhibitors at IC_{50} concentrations, and compared to vehicle treatment with DMSO. Compounds were added to embryo water after 6 hours post-fertilization (hpf) to examine the effects of these compounds on embryos that will be harboring tumor xenografts upon transplantation at 48-72 hpf and establish background fluorescence for treated embryos in the absence of human tumor cells. Treatment compounds, when used at IC_{50} concentrations had no notable toxic effects. At least 20 embryos were used in each treatment. *B*, Survival of fish embryos upon treatment with C-209 and chemotherapy. Data are from two independent experiments utilizing 200 embryos per group.

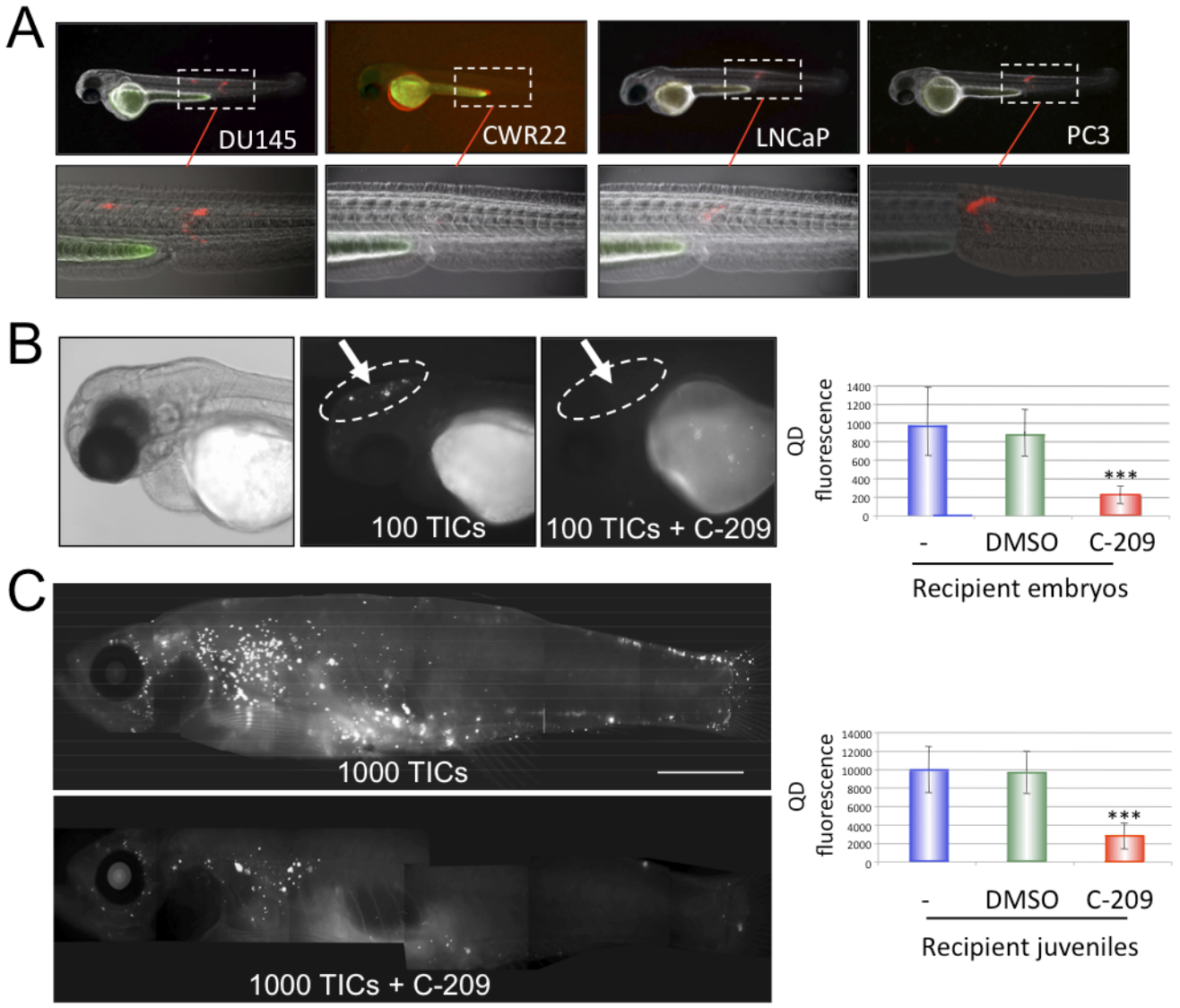

Figure S12. Anti-tumor activity of BMI-1 inhibitors. *A*, Representative images of embryos transplanted SC in the tail region with Q-dots-labeled rapidly adherent $CD49b^{hi}CD29^{hi}CD44^{hi}$ (TICs) CWR22, LNCap, PC3, DU145 cells. Non-tumorigenic normal prostate cells were used as control and yielded no tumor formation. Images are overlays of bright field, GFP and red 605 fluorescent images from embryos that developed localized tumors with images taken during tumor development at 4 dpt. *B*, Transplantation of 10 TICs resulted in brain metastasis in zebrafish embryos (arrow in outlined area). Exposure of the same embryo to the BMI-1 inhibitor C-209 at 2 μM in the water for 72 hours reduces the size and fluorescence emitted by DU145 cells growing in zebrafish embryonic brain (compare circled areas before and after treatment). Bright field image of this treated embryo is corresponding to the fluorescent image after treatment. Right graph demonstrates the QD fluorescence emitted by the tumor masses in outlined tumor regions of either untreated, vehicle, or C-209 treated embryos that were measured and displayed in arbitrary fluorescence units reflecting tumor growth or regression after treatment for 72 hours. Data represent 8 independent experiments displayed as mean ± S.D. derived from three replicate experiments using ≥20 embryo/group (*$p<0.001$). *C*, Florescent composite images of whole juvenile zebrafish recipients transplanted with DU145 TICs. Images are lateral views with the head to the left. Transplantation of 500 TICs in conditioned juvenile zebrafish resulted in tumor growth, widespread migration, and metastasis of QD-labeled tumor cells throughout the fish. Treatment with C-209 at 2μM in conditioned water for 5 days reduced the size and fluorescence emitted by DU145 cells. The graph demonstrates QD fluorescence emitted by tumor masses in juvenile fish that are either untreated, vehicle or C-209 treated that were measured, and displayed in arbitrary fluorescence units reflecting tumor growth or regression. Data are displayed as mean ± S.D. derived from three experiments using 3 juvenile fish/group (*$p<0.001$).

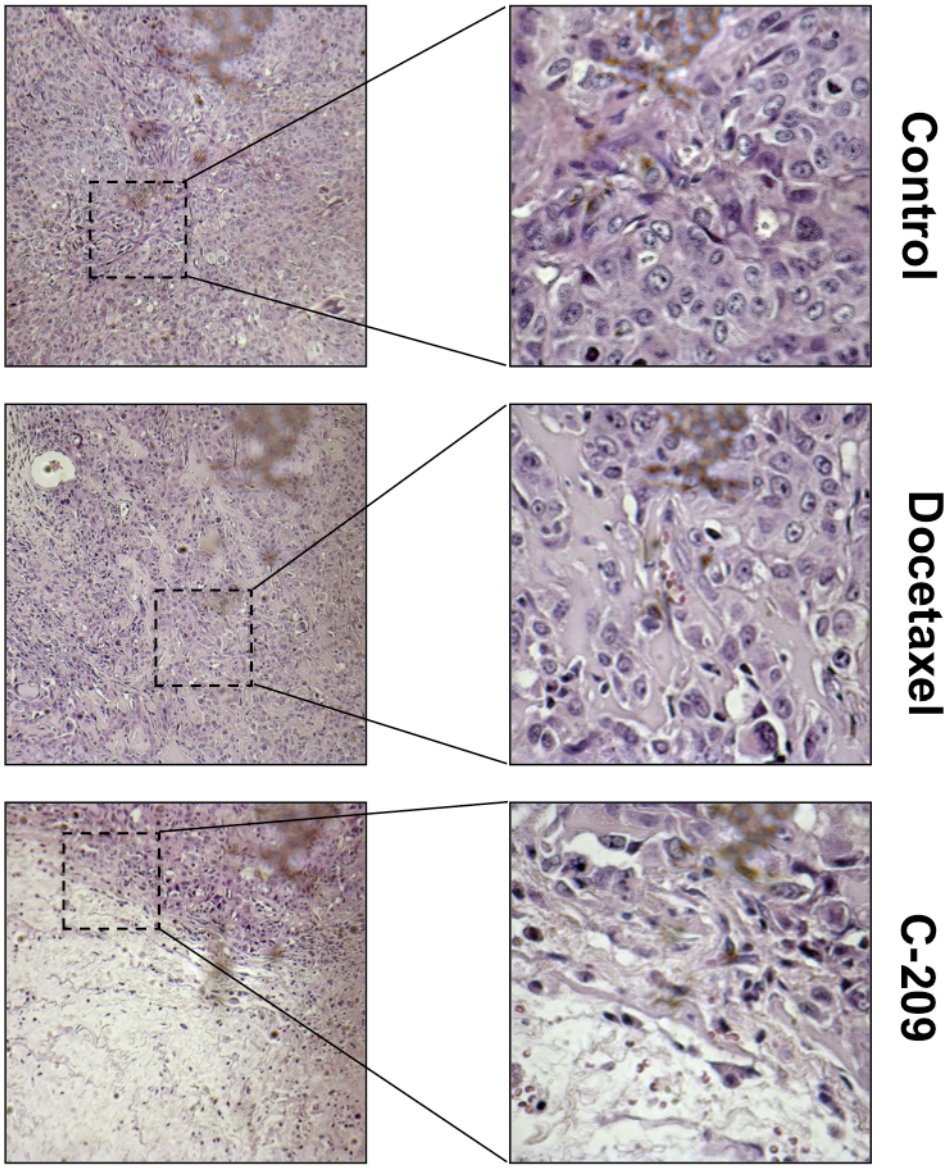

Figure S13. Representative H&E staining of mouse xenograft sections indicating the histological effects of treatments.

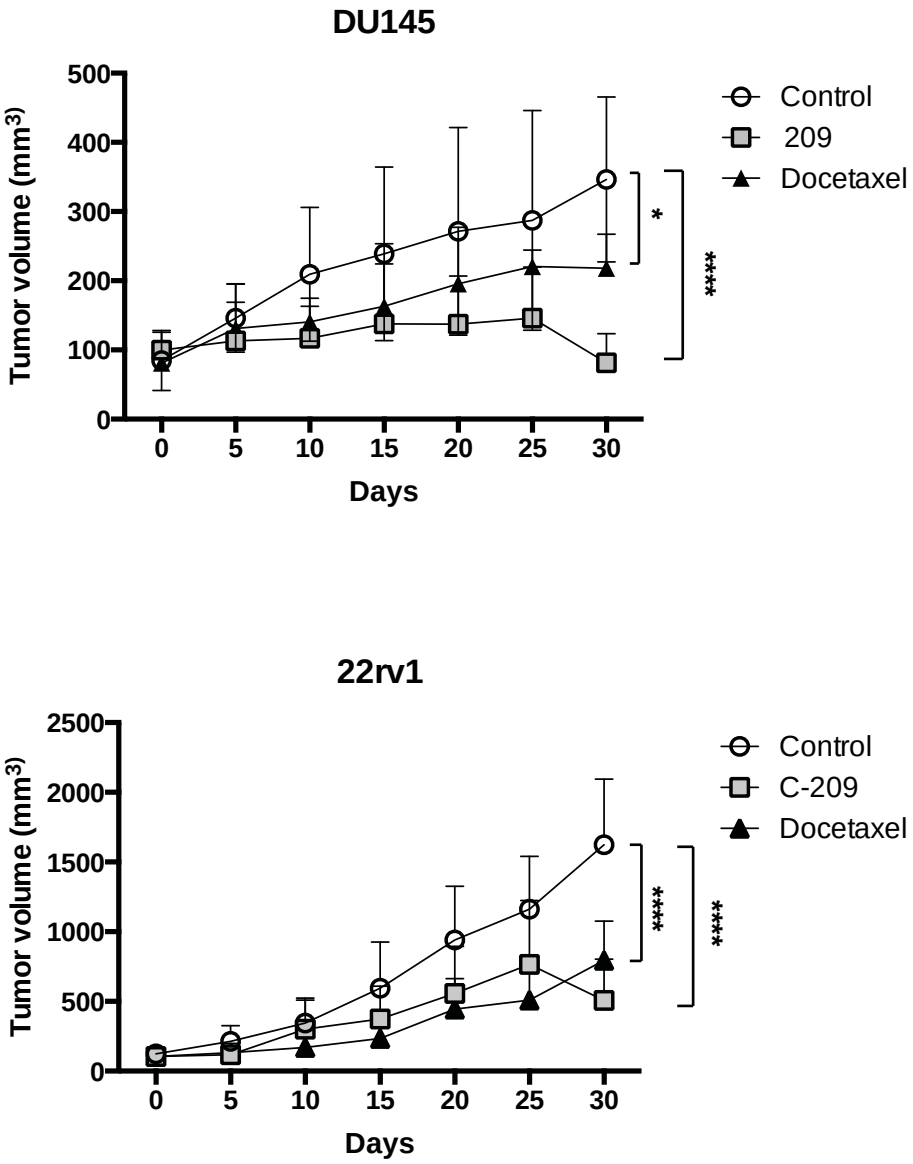

Figure S14. *In vivo* pharmacological targeting of BMI-1 in androgen independent DU145 and androgen sensitive 22rv1 PCa mouse xenografts. Growth rate of mouse xenografts generated after subcutaneous (SC) injection. Mice were randomized and administered daily with 60 mg/kg/day of C-209 for twelve days and docetaxel 6mg/kg once a week for two consecutive weeks. Results are mean ± S.D. of two independent experiments. Comparison of tumor volumes between the three groups was determined by two-way ANOVA with Bonferroni post-hoc test. Graph indicates significance of Docetaxel *vs.* Control at day 30 (**p<0.01) and C-209 *vs.* Control at day 30 (****p<0.0001). In each experiment, n=8/group.

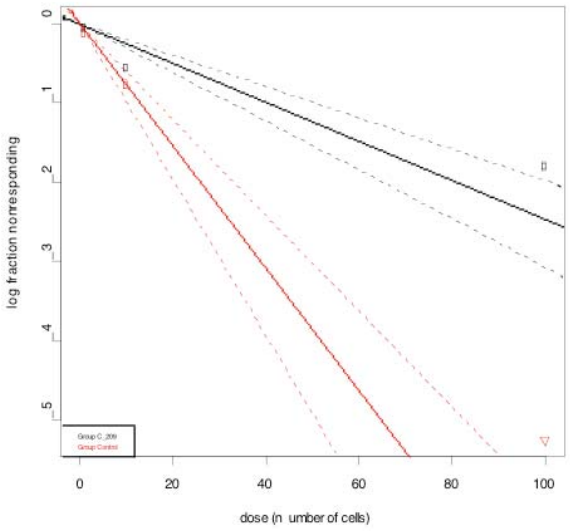

Confidence intervals for 1/(stem cell frequency)

	Lower	**Estimate**	Upper
Control	16.5	**12.9**	10.2
C-209	50.6	**40.6***	32.6

Differences in stem cell frequencies between the groups. *P value equals 4.9^{e-12}.

	Colony Formation	
Number of cells plated	**Control**	**C-209**
1	10/96	3/96
10	51/96	40/96
100	96/96	80/96

Figure S15. Colony-formation frequency evaluated by dilution analysis of xenograft-derived cells from untreated mice and mice treated with C-209 60mg/kg/day. Data were analyzed using ELDA software (http://bioinf.wehi.edu.au/software/elda/). Upper panel: A log-fraction plot of the dilution model fitted to the data in the lower table. The slope of the line is the log-active cell fraction. The dotted lines give the 95% confidence interval. The data value with zero negative response at corresponding dose is represented by a down-pointing triangle.

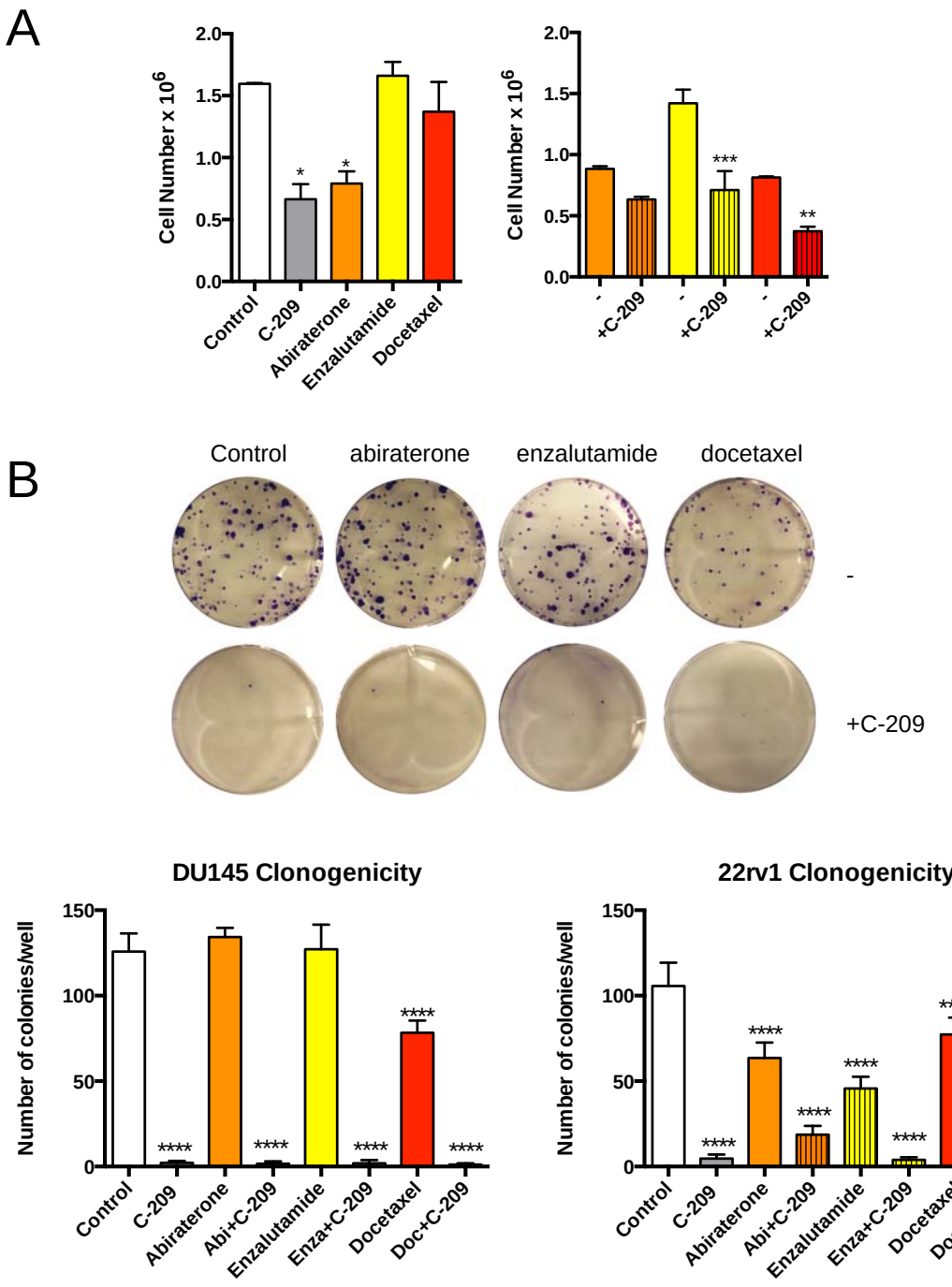

Figure S16. BMI-1 inhibition effects on androgen-dependent and -independent cells. *A,* Cell proliferation of 22rv1 cells treated with C-209 (2μM), abiraterone (5μM), enzalutamide (5μM) and docetaxel (2.5nM) for 72 hrs (right panel). Left panel is showing cell survival of therapy-resistant cells. Cells, pre-treated with abiraterone (5mM), enzalutamide (5mM) and docetaxel (2.5nM) for 72 hrs were washed and remaining cells were exposed to C-209 (2μM) for another 3 days. Graphs are showing results indicated as mean ± S.D. of two independent experiments with *p<0.05, **p<0.01, ***p<0.001. *B,* Representative images of DU145 colony-forming ability of cells pre-treated as indicated above (upper panel). Lower panel is showing average number of colonies/plate for each treatment mean ± S.D. of two independent experiments with 6 wells/condition. ****p<0.0001 as compared to untreated Control.

Supplementary Methods

Western blot (WB) analyses

Pelleted cells were lysed and 50 μg of total proteins were separated on SDS PAGE gels and analyzed using: mouse monoclonal anti-BMI-1 clone F6 against the N-terminal (1:1000) (Millipore, rabbit polyclonal anti-BMI-1 SDI against the C-terminal (1:2,000) (SDI), mouse monoclonal anti-ubiquityl (γ)-histone H2A clone E6C5 (1:1,000) (Millipore), rabbit polyclonal anti-H2A (total) (1:1,000) (Millipore), anti-β-tubulin (1:5000) (Millipore), rabbit polyclonal anti-β-actin (1:10,000) (Rockland) and rabbit polyclonal anti-vinculin (1:1000) (Cell Signaling).

Genetic modulation of BMI-1 expression

For BMI-1 knockdown, DU145 cells were transfected with GIPZ Bmi-1 shRNA construct (Open Biosystems) using lipofectamine. Bmi-1 shRNA positive cells were selected in media with 0.5 mg/ml of puromycin. Selection was carried out in the presence of puromycin 5 μg/ml (Sigma). For BMI-1 overexpression, HEK 293T cells were transfected with pMcs-Bmi1-IRES-GFP retroviral vector along with packaging plasmids using the calcium phosphate method. The viral supernatant was used to infect DU145 cells, which were then selected through EGFP expression by cell sorting.

Migration assay

Cell migration was assessed in 24-well transwell boyden chambers (Costar Scientific Corporation, Cambridge, MA). PCa cells treated with docetaxel (2.5nM) and C-209 (2μM) for 96h were washed twice and replated in fresh medium without treatments for an additional 3 days. Consequently, $2x10^4$ cells/well were suspended in complete growth medium and placed into upper chambers. After 24 hrs, migrated cells were stained with Comassie Brilliant Blue and counted under the microscope.

Soft agar colony forming assays

To evaluate the fraction of self renewing cells, 500 cells were plated in the top agar layer in each well of a 24-well culture plate with 0.3% top agar layer and 0.4% bottom agar layer (SeaPlaque Agarose, Cambrex, NJ). Cultures were incubated at 37°C for 20 days. Colonies were stained after 3 weeks with crystal violet (0.01% in 10% MetOH), visualized and counted under microscope and photographed. For DU145 and RWPE colony formation assay, cells were treated with DMSO and C-209 (1μM, 2μM, 4μM, 8μM, 12μM). Colonies were enumerated over a period of 2 weeks. To perform clonogenic assay in soft agar *ex vivo,* DU145 Luc2EGFP xenograft-derived cells were isolated once tumors were aseptically removed and dissociated. Cells recovered were extensively washed and sorted for EGFP expression; next, 500 fluorescent cells for each treatment condition were plated as described above. After 20 days, colonies were visualized and counted.

Soft agar colony forming assays were carried out for primary PCa cells pre-treated with docetaxel (2.5nM) and C-209 (2μM) for 96h. Next, cells were collected, washed and replated in fresh medium in the absence of treatments for additional 3 days. Subsequently, cells were washed and 500 single cells were plated in the top agar layer in each well of a 24-well culture plate with 0.3% top agar layer and 0.4% bottom agar layer (SeaPlaque Agarose, Cambrex, NJ). Cultures were incubated at 37°C for 20 days. Colonies from triplicate wells were stained with crystal violet (0.01% in 10% MetOH), visualized and counted under microscope and photographed. Colony forming assays were carried out for DU145 and 22rv1 PCa cells pre-treated with abiraterone (5μM), enzalutamide (5μM) and docetaxel (2.5nM) for 72 hrs. Subsequently, cells were washed and exposed to C-209 (2μM) for an additional 3 days. Survived cells were washed, counted and 200 cells /each condition were plated for clonogenic assessment.

Cell viability assays

For chemosensibility studies, 5 x10^3cells/well control vector-transduced (Sh-Scr) and BMI-1-depleted (shBMI-1) cells were plated in 96-well plates and treated with Docetaxel (2.5nM) or metotrexate (10nM) or the following concentrations of C-209: 0.0195, 0.0391, 0.0781, 0.1560, 0.3125, 0.6250, 1.25, 2.5, 5, 10, and 20 μM

for 72hrs. Cell viability was always evaluated after 72hrs through MTS assay (Promega) following manufacturer's instructions. For cell survival assays, primary and immortalized PCa cells were treated with docetaxel (2.5nM), enzalutamide (5μM), abiraterone (5μM) or C-209 (2μM) for 4 days. Next, cells were collected, washed and replated in fresh media without treatments for an additional 3 days. On day 7, cells were collected and counted by Trypan Blue exclusion and, when required, plated for clonogenic assays.

Overcoming therapy-resistance assay.

To assess the effects of C-209 on therapy-resistance cells, DU145, LNCaP and 22rv1 PCa cells were treated with docetaxel (2.5nM), enzalutamide (5μM) and abiraterone (5μM) alone for 4 days. Next, remaining living cells were collected, washed and replated in fresh media with or without C-209 (2 μM) for an additional 3 days. On day 7, cells were collected and counted by Trypan Blue exclusion.

Cytotoxicity assays

Cytotoxicity of C-209, C-210, and C-211 compounds (PTC therapeutics) and methotrexate, doxorubicin and docetaxel were assayed following a 3-day exposure. DU145 Cells (3×10^3 cells/well) were treated with multiple concentrations to determine an IC_{50}, and toxicity analyzed using MTS assay (Sigma) per manufacturer's instructions. IC_{50} concentrations were determined using Hill's equation in Graph-Pad prism 4.0 software.

β-gal assay for senescence

Senescence experiments were performed in two 6-well plates for each treatment. Percentage of senescent cells was determined based on counts of 1,000 cells per treatment. Treatments with BMI-1 inhibitors were carried on for 72h. Subsequently, cells were washed and fixed in 4% paraformaldehyde, washed in PBS pH 7.4 followed by PBS pH 6.0 for one hour each. Fixed cells were then stained with 2μg/ml x-gal (Sigma) overnight at 37°C and washed with PBS pH 6.0. Cells were imaged and staining was quantitated using Adobe Photoshop and ImageJ. The β-gal staining intensity was measured using the average intensity density of hue saturation.

In vitro prostasphere assay

Prostate tumor cell spheroid assay from cells lines was performed based on established methods (1-3), while we (4) and others (5-7) have previously described the spheroid assay from primary human prostate cancer cells. Prostate cells were counted and re-suspended at 2 x 10^3 cells/well in KSFM media and plated on 1% agarose coated plates. The cellular suspension was then plated in the well on 12-well plates and incubated at 37°C for 30 min. One milliliter of defined media was then added to each well and plates were replaced in 37°C incubator. For dissociation and passage of prostaspheres, incubation for one hour in 1 mg/ml Dispase (Invitrogen) was performed. Spheres were collected, washed in RPMI, and trypsinized (TripLE 200microliters/12-well plate). Every 3 days, half of the media was replaced and prostaspheres of >50 μm in diameter and consisting of >50 cells were counted on day14. Prostate cells obtained from dissociated primary prostaspheres remained viable after freeze/thaw, with formation of new prostaspheres that could be serially passaged. Dissociated prostaspheres could be passaged >3 generations. Single cells from day-7 prostaspheres were used in secondary and tertiary spheroid assays, and secondary or tertiary prostaspheres with size and morphological features similar to primary prostaspheres were counted.

Docking of C-209 to the human BMI-1 RNA

The interaction energy scores (E_{int}) are used to estimate the binding energy in the UCSF DOCK scoring of C-209 with BMI-1 RNA (8). The docking was performed keeping the RNA structure rigid while permitting flexibility and full rotation and translation in the small molecule (8). The imidazo-pyrimidine ring of C-209 mimics the purine ring of guanine, therefore, guanine was used as a reference. UCSF DOCK scores were E_{vdw} (kcal/mol), E_{elec} (kcal/mol), and E_{int} (kcal/mol), were generated using the following equation: $E_{int} = E_{vdw} + E_{elec}$. The lower the interaction energy score; the more stable the complex contacts with the RNA due to complete fitting into the binding pocket. C-209 UCSF DOCK scores were E_{vdw} (kcal/mol) -60.6, E_{elec} (kcal/mol) -5.2, and E_{int} (kcal/mol) -65.8, as compared to guanine scores of E_{vdw} (kcal/mol) -36.4, E_{elec} (kcal/mol) -4.1, and E_{int} (kcal/mol) -40.5, respectively, when $E_{int} = E_{vdw} + E_{elec}$. The lower the interaction energy score; the more stable the complex (9).

Therefore, C-209 is predicted to form the most stable complex with BMI-1 RNA. Guanine has a higher E_{vdw} energy owing to its inability to have more van der Waals contacts with the RNA due to its smaller and less complete fitting into the binding pocket.

Flow cytometric analysis

Cells were treated with C-209 2μM. After 72hrs, treated and untreated cells were stained with a propidium iodide (PI) staining solution (trisodium citrate 0.1%, NaCl 9.65μM, NP40 0.3%, PI 50μg/ml and RNase A 200μg/ml) for 30 min at RT. Cell cycle profile was acquired with a BD FACSCalibur flow cytometer (Becton Dickinson) and analyzed with FlowJo software (Tree Star Inc.; http://www.flowjo.com/index.php).

Cell sorting

For cytofluorimetric analyses, PCa cells were washed in 1xPBS, 2% FBS and 0.01% sodium azide and stained with isotype controls or anti-CD49B-Pacific Blue (Biolegend) and anti-CD44-PE/CD29-APC (BD). Cells were also stained with 7AAD to exclude dead cells. The effects of C-209 (2μM) on CD44 and CD49b/CD29 expression were assayed in DU145, PC3 and CWR22 and patient-derived cells (Patients # 28869, 33020, 33120, 33072, and 33106) after 72hrs of treatment. Acquisitions were made using a BD FACSCalibur flow cytometer (Becton Dickinson, Franklin Lakes, NJ) and analyzed using cell quest software. Cell sorting was performed on cells stained with CD44-APC or CD49b/CD29-FITC and sorted using Influx High Speed Cell Sorter (BD Biosciences). Sorted cells were washed with PBS and treated as needed for the different experiments.

$CD34^+$ and DU145 colony forming assay

$CD34^+$ cells were isolated from cord blood samples (Elie Katz umbilical cord blood banking center, NJ) using MACS magnetic column separation system (Miltenyi). Briefly, cells were magnetically labeled with $CD34^+$ microbeads, and run twice through magnetic columns to increase purity. Cell viability and purity were assessed by flow cytometry. Purified $CD34^+$ cells were supplemented with IL-3, rhTPO (Kirin brewery), and FLT3-L (Peprotech) cytokines. Cells were suspended at 3 x 10^3 concentration in one ml of methocult (Methocult GF

H4434; Stem cell technologies). Both $CD34^+$ and DU145 cells were treated with DMSO and C-209 (1μM, 2μM, 4μM, 8μM, 12μM). Colonies were enumerated over a period of 2 weeks.

Microscopy and peripheral blood analyses

To evaluate bone marrow cellularity, histologic sections were stained with hematoxylin/eosin. For May-Grünwald-Giemsa staining, mice were sacrificed at the end of the treatment, femurs were harvested and marrow flushed with a 23G (0.45 × 10 mm) syringe needle to collect single-cell suspensions. Bone marrow sections and blood May-Grünwald-Giemsa–stained cells were analyzed with a Zeiss Axiostar Plus microscope equipped with an A-Plan 10× dry objective (numerical aperture: 0.25) and an A-Plan 100× oil objective (numerical aperture: 1.25), respectively (Zeiss). Images were taken with a Canon Power Shot G9 camera. Peripheral blood was obtained from cardiac puncture bleeding of mice treated with either vehicle or C-209 60mg/kg/day for 2 weeks. Blood was dripped directly after removal into tubes containing 0.5 mol/L EDTA. Peripheral blood parameters were analyzed at a reference hematology laboratory (ANTECH Diagnostics) within 4 hours from bleeding.

Immunohistochemistry

For IHC, fixed paraffin-embedded tissue samples from human prostate tumors were stained with anti-BMI-1 antibody (Cell Signaling) following antigen retrieval. Sections were scored for percentage of positive cells as well as intensity on a 0-3 scale by pathologists blinded to treatment. Slides were analyzed with a Zeiss Axiostar Plus microscope equipped with an A-Plan 10× dry objective (numerical aperture: 0.25) and images were taken with a Canon Power Shot G9 camera.

Zebrafish Drug Treatments

The following compounds were diluted in egg water: C-209, Cycloheximide (CHX), Docetaxel, Methotrexate (MTX), DMSO, and Ethanol. For all treatments, fish were incubated at the normal maintenance temperature of

28.5°C for a 3-days toxicity test. Viable embryos staged at 12 hours post fertilization (hpf) were counted into 12-well plates; all egg water removed and 2mL of treatment water added. Bright field images were taken on 1dpf, 2dpf and 3dpf with a Canon Powershot digital camera adapted to a Zeiss Stemi 2000-C microscope. Six-week old zebrafish were placed in 4ml treatment water (drug diluted in fish system water) at 2 fish per well in a 12-well plate. For adults only treatment water was changed daily due to debris accumulation in the wells.

Transplantation of human prostate cancer cells in zebrafish

Cells were resuspended in 0.5x Dulbecco's PBS (DPBS) containing QD605 (red fluorescence) (QD605; Invitrogen) and lipofectamine at a ratio of 1:2 for 2 hours. Cells were suspended in 0.5x DPBS for transplantation into dechorionated and anesthetized (0.5x tricaine methanesulfonate, MS-222; Sigma) 48-hour post fertilization (hpf) embryos using 15 μm (internal diameter) injection needles. Injections were either subcutaneously (SC), or above the yolk into the sinus venosus using a Celltram microinjector. After transplantation, embryos were incubated for 2 hours at 37°C, and were then maintained in a humidified incubator at 33°C. Human cells were monitored under fluorescent microscopy for homing and tissue repopulation.

Limiting dilution assay

Limiting dilution assays were performed on EGFP-sorted xenograft-derived cells. Briefly, xenografts from C-209 treated and untreated mice were removed and enzymatically dissociated. Recovered cells were extensively washed and sorted for EGFP in order to exclude any non human tumor cells; subsequently cells were plated at the density of ~1, 10, 100 and 1000 cells/well in 96-well plates under standard growth conditions. After 14 days, colonies were fixed and stained (20% methanol fixation followed by 0.1% crystal violet staining). Clonogenic capability was assessed visually under the microscope. Wells containing no colonies were excluded for the analysis. Tumor-formation frequency was evaluated by using Extreme Limiting Dilution Analysis (ELDA) software (http://bioinf.wehi.edu.au/software/elda/index.html).

Supplementary References

1. Essand M, Nilsson S, Carlsson J. Growth of prostatic cancer cells, DU 145, as multicellular spheroids and effects of estramustine. Anticancer Res 1993;13:1261-8.

2. Sgouros G, Yang WH, Enmon R. Spheroids of prostate tumor cell lines. Methods Mol Med 2003;81:79-88.

3. Tokar EJ, Ancrile BB, Cunha GR, Webber MM. Stem/progenitor and intermediate cell types and the origin of human prostate cancer. Differentiation 2005;73:463-73.

4. Bansal N, Davis S, Tereshchenko I, et al. Enrichment of human prostate cancer cells with tumor initiating properties in mouse and zebrafish xenografts by differential adhesion. Prostate 2014;74:187-200.

5. Goldstein AS, Lawson DA, Cheng D, Sun W, Garraway IP, Witte ON. Trop2 identifies a subpopulation of murine and human prostate basal cells with stem cell characteristics. Proc Natl Acad Sci U S A 2008;105:20882-7.

6. Garraway IP, Sun W, Tran CP, et al. Human prostate sphere-forming cells represent a subset of basal epithelial cells capable of glandular regeneration in vivo. Prostate 2010;70:491-501.

7. Guo C, Zhang B, Garraway IP. Isolation and characterization of human prostate stem/progenitor cells. Methods Mol Biol 2012;879:315-26.

8. Shoichet BK, McGovern SL, Wei B, Irwin JJ. Lead discovery using molecular docking. Curr Opin Chem Biol 2002;6:439-46.

9. Pettersen EF, Goddard TD, Huang CC, et al. UCSF Chimera--a visualization system for exploratory research and analysis. J Comput Chem 2004;25:1605-12.